AD

REPORT R-1806

LOW CYCLE FATIGUE CRACK PROPAGATION CHARACTERISTICS OF HIGH STRENGTH STEELS

by

CARL M. CARMAN
JESSE M. KATLIN

April 1966

AMCMS Code 5025.11.294

Distribution of this report is unlimited.

UNITED STATES ARMY
FRANKFORD ARSENAL
PHILADELPHIA, PA.

DISPOSITION INSTRUCTIONS

Destroy this report when it is no longer needed. Do not return it to the originator.

The findings in this report are not to be construed as an official Department of the Army position unless so designated by other authorized documents.

BLANK PAGE

REPORT R-1806

LOW CYCLE FATIGUE CRACK PROPAGATION CHARACTERISTICS OF HIGH STRENGTH STEELS

by

CARL M. CARMAN
JESSE M. KATLIN

AMCMS Code 5025.11.294
DA Project 1C024401A328

Pitman-Dunn Research Laboratories
FRANKFORD ARSENAL
Philadelphia, Pa. 19137

April 1966

FOREWORD

The work described in this report is part of the continuing effort in the study of fracture properties of high strength materials. The authors wish to thank Dr. Paul C. Paris, of Lehigh University, for his assistance during the investigation and review of the final paper, and Miss Marie Dougherty and Mrs. Mary Schuler, of Frankford Arsenal, for their work in conducting the mechanical tests and electron microscopy.

ABSTRACT

The fatigue crack growth properties of various high strength steels, including the 250 and 300 grades of the 18Ni-Co-Mo maraging steel, H11 steel, and D6A steel, have been studied using a center-cracked specimen. Experiments were conducted by cycling either at a constant stress or at a constant value of the stress intensity parameter, K.

A log-log plot of da/dN as a function of K for these steels resulted in a straight line having a slope of four. The data exhibited normal scatter about this straight line. These data are in agreement with the relationship $da/dN = (\Delta K)^4/M$ as proposed by Paris. A departure from this relation to higher rates was observed at values of cyclic K equal to 0.7 to 0.8 of static K_c.

Electron microfractographs taken along the path of fatigue crack extension in the 250 grade maraging steel showed the growth ring pattern characteristic of fatigue. Measurement of the growth ring spacings and knowledge of the crack length permit calculation of the rate of crack extension as a function of K. The rates of crack extension, as determined by fractography and actual measurement on the specimen, are in good agreement.

A technique for calculating the cyclic life of structures involving a numerical integration of K as a function of crack length and stress was programmed for computer operation. This calculation allows for the change in slope of the K vs da/dN at higher values of cyclic K. The results of these calculations are compared with the life prediction made by simple mathematical integration of the fourth power relationship for an infinite plate.

TABLE OF CONTENTS

List of Tables

List of Illustrations

GLOSSARY

a = one-half crack length

a_{cr} = half crack length at instability

a_o = initial half crack length

B = specimen thickness

C = constant

C_1 = constant = $2\pi/M$

K = parameter describing the local elevation of the elastic stress field ahead of the crack

K_c = fracture toughness of a material

K_{Ic} = plane strain fracture toughness of a material

m = exponent

M = material constant

n = exponent

N = number of cycles

N_F = number of cycles to failure

W = specimen width

γ = exponent in crack propagation law

ΔK = range of K

σ = gross section stress

σ_{ys} = 0.20 percent yield strength

INTRODUCTION

The development of lightweight high strength structures has directed attention toward the utilization of steels having yield strengths in excess of 200,000 psi. These materials exhibit tendencies toward low stress failures in the presence of defects. To efficiently use these steels, the size of defects which will cause failure should be known.

In the case of most high strength materials, the defect size for instability at a given stress level may be estimated by the methods of fracture mechanics. Fatigue is responsible for a high percentage of structural failures; therefore, there is considerable interest in this area. However, these calculations give little insight into either the rate of fatigue crack propagation or the mechanism involved. More detailed information concerning the rate of crack propagation is necessary to estimate the cyclic life of a structure.

The fracture toughness of the material defines the size of the defect which will cause failure under a given stress, and this defect can usually be detected by careful use of nondestructive techniques. In certain structures, however, the rate of fatigue crack extension may be the limiting factor in design, rather than the fracture toughness, per se, of the material. If the cyclic stress to which a structure may be subjected is relatively high (approximately one-half the yield strength), then the rate of growth of subcritical size defects to a critical size can be so rapid that either the operating stress must be reduced or a limit set on the useful cyclic life of the structure.

Although considerable fatigue data have been accumulated for this class of materials, most of these data are of the rotating beam endurance limit type and are not interpretable in terms of the crack propagation characteristics of the material. This study was undertaken, therefore, to investigate the low cycle, or early stages, of fatigue crack propagation characteristics of these materials in order to supply the needed data in this area.

PROCEDURE, RESULTS, AND DISCUSSION

The high strength steels selected for this investigation were: H11 steel, D6Ac steel, 250 grade maraging and 300 grade maraging steels. These steels were heat treated by conventional techniques to the strength levels normally employed in high strength-to-density structural applications.

The engineering tensile properties of the steels considered were determined, using a pin-loaded strip type tensile specimen having a 0.500 inch wide gage section and a two-inch gage length. The tensile properties of these steels were given in Table I.

TABLE I. Tensile Properties of Steels Investigated

Material	Direction	Strength (psi) Yield 0.20% Offset	Strength (psi) Tensile	Elongation (%)
H11	Longitudinal	242,500	305,500	7.4
	Transverse	242,300	307,200	7.3
D6Ac	Longitudinal	241,500	271,500	7.0
250 Maraging				
0.075	Longitudinal	267,900	275,000	3.2
0.075	Transverse	278,300	285,000	2.6
0.250	Longitudinal	252,000	266,000	7.6
300 Maraging				
0.075	Longitudinal	285,800	290,300	3.2
0.250	Longitudinal	295,000	302,600	4.1

The center-cracked specimen shown in Figure 1 was used to determine the fracture toughness properties of the material and to study the fatigue crack propagation rates. The plane strain fracture toughness was determined using the "pop-in" technique, described by Boyle, Sullivan, and Krafft.[1*] These data are summarized in Table II.

The fracture toughness was considerably higher for the thinner plates of D6Ac steel and the 250 and 300 grade maraging steels, than for the thicker specimens. This type of behavior is in accord with the fracture mode transition analysis as proposed by Irwin.[2] He found that the fracture toughness of very thick specimens is relatively low and corresponds to the plane strain fracture toughness. Moreover, the fracture toughness increases as the plate thickness decreases, until a maximum of fracture toughness is obtained. This behavior has been correlated with the size of the plastic zone relative to the plate thickness, with the maximum occurring when the plastic zone size is approximately equal to the plate thickness.

Since 1953, considerable attention has been directed toward the development of crack propagation laws. Based on earlier work of Head,[3] Frost and Dugdale,[4] and Liu,[5] it was found that these laws are often expressed in the general form shown in the following equation.

*See REFERENCES.

TABLE II. Fracture Toughness of High Strength Steels

Material	Direction	W (in.)	B (in.)	Stress at "Pop-in" (psi)	a_o (in.)	K_{Ic} (psi/in.)	Stress at Failure (psi)	a_{cr} (in.)	K_c (psi$\sqrt{in.}$)
H11	Longitudinal	3.00	0.079	38,900	0.430	47,000	49,000	0.485	63,200
	Transverse	3.00	0.080	34,800	0.422	42,400	44,500	0.460	54,800
D6Ac	Longitudinal	3.00	0.166	42,400	0.410	54,800	57,000	0.521	78,500
	Transverse	3.00	0.164	40,700	0.460	49,700	47,400	0.550	67,000
	Longitudinal	3.00	0.075	-	-	-	103,000	0.508	143,200
	Transverse	3.00	0.077	-	-	-	118,700	0.538	163,200
250 Maraging	Longitudinal	4.00	0.278	50,700	0.618	73,600	66,600	1.000	133,000
	Longitudinal	4.00	0.070	87,500	0.544	70,400	139,500	0.700	218,400
300 Maraging	Longitudinal	3.00	0.271	22,800	0.505	43,200	47,700	0.771	84,300
	Longitudinal	3.80	0.074	-	-	-	124,800	0.678	191,400
	Transverse	4.00	0.074	-	-	-	127,400	0.639	188,500

Code: a_{cr} = Half crack length at instability
a_o = Initial half crack length
B = Specimen thickness
K_c = Fracture toughness of a material
K_{Ic} = Plane strain fracture toughness of a material
W = Specimen width

$$\frac{da}{dN} = \frac{\sigma^n a^m}{C} \tag{1}$$

where a = one-half crack length
C = constant
m = exponent
n = exponent
N = number of cycles
σ = gross section stress.

The expression for the stress intensity parameter, K, in a uniformly stressed infinite plate is given in

$$K = \sigma\sqrt{\pi a} \tag{2}$$

By combining Equations 1 and 2, one may express the rate of fatigue crack propagation as a function of K, and this is advantageous since K reflects the effect of external load and configuration on the intensity of the stress field around a crack tip. Since the crack tip stress field has the same form for various configurations, a correlation of fatigue crack growth between various specimen geometries is possible.

Crack growth rate determinations were made using two load-programing techniques: (1) cycling at a constant value of K by appropriately varying the stress with changes in crack length; and (2) cycling at a constant stress with accompanying variations of K due to increasing crack length. The constant K technique was used for evaluating crack growth rates in the high K level area (above 0.7 K_c), and the constant stress technique was used for tests which started in the low K area. Sufficient overlap of data was provided in the range where the K levels were similar to insure a smooth transition between the two methods of testing.

The high stress fatigue tests conducted at a constant value of K were performed on a universal testing machine. The initial crack length (notch length plus fatigue crack) in the specimen was measured with a traveling microscope. The precision of the microscope was ±0.0001 inch, and the accuracy of measurement of the total crack length was approximately ±0.002 inch. The value of load required to produce a given K value was computed by solving the following equation[6] for σ.

$$K = \sqrt{\sigma^2 W \tan\left(\frac{\pi a}{W} + \frac{K^2}{2W\sigma_{ys}{}^2}\right)} \tag{3}$$

The specimen was loaded in uniaxial tension to the calculated value of load, held for three minutes, the surface crack length measured, and then the load released. The measured crack length was used in Equation 3 to compute the new value of load which would reproduce the same value of K in the next cycle. The cycle was then repeated.

The low stress fatigue tests were conducted using an Amsler tension-tension hydraulic machine. In these experiments, the maximum load for each specimen was held constant and the minimum tensile load was maintained as low as possible with the equipment, but never less than 1000 pounds. Crack lengths were measured periodically, using a traveling microscope. Typical crack growth curves for the various materials are shown in Figures 2 to 7, incl.

The rate of crack growth, da/dN, under constant stress conditions was determined by halving the slope of the 2a vs N curve at a given point. The value of "a" at that point and the stress were used to calculate K. For cracks equal to or less than W/2, Equation 3 was used to calculate K.

The tangent equation (Equation 3) developed by Irwin, although containing a plastic zone correction, tends to become inaccurate at relatively long cracks ($2a \geq W/2$). The equation developed by Greenspan[7] is felt to be a better approximation for K for longer cracks, even though it does not incorporate the plastic zone correction. Therefore, the values of K for longer cracks were calculated using

$$K = \sigma \sqrt{\pi a}\, \alpha \tag{4}$$

where

$$\alpha = \frac{\left[4 + 2\left(\frac{2a}{W}\right)^4\right]^{1/2}}{2 - \left(\frac{2a}{W}\right)^2 - \left(\frac{2a}{W}\right)^4}$$

In Figure 8, the rate of crack extension in H11 steel is plotted as a function of K. Similar data for D6Ac are shown in Figure 9, and the data for the maraging steels are shown in Figures 10 through 13. Examination of these data shows that, at low values of cyclic K, the data conform to a straight line plot. This would suggest that the rate of crack extension may be expressed as a function of K and is shown in the following equation (proposed by Paris and Erdogan).[8]

$$\frac{da}{dN} = \frac{\Delta K}{M} \tag{5}$$

Comparison of the slopes of the experimental curves with calculated values shows that a value of the exponent, γ, equal to four gave best agreement over the range of experimental data. For comparison purposes, lines having γ values of four (slope = 1/4) are shown on Figures 8 to 13.

In order to gain further insight into the mechanism of crack propagation, and to provide additional information on the rate of crack propagation, electron microfractographs were prepared at selected positions

along the path of fatigue crack extension. Two-stage faxfilm replicas, shadowed with carbon, were used for this phase of the investigation. Typical fractographs for the 250 grade maraging steel are shown in Figures 14 and 15.

These fracture surfaces exhibited fatigue growth rings (striations) similar to those reported by Pelloux[9] for high strength aluminum alloys. Recent work by Hertzberg and Paris[10] and Schuler and Carman[11] have shown that a quantitative relationship exists between the rates of fatigue crack propagation observed microscopically and macroscopically. Therefore, measurement of the spacing from one growth ring to the next represents the extent of crack growth per cycle of loading. (Typical growth rings are indicated by the arrows on Figures 14, 15, and 16.) These data are summarized in Table III. It will be observed that the crack growth rates determined by these two methods are in close agreement.

TABLE III. Comparison of Crack Growth Rates as Determined Macroscopically and Microscopically

K ($psi\sqrt{in.}$)	da/dN (in./cycle)	
	Macroscopic	Microscopic
38,000	1.11×10^{-5}	1.12×10^{-5}
41,000	1.49×10^{-5}	1.41×10^{-5}
44,200	1.68×10^{-5}	1.41×10^{-5}
47,400	2.15×10^{-5}	2.18×10^{-5}
48,000	2.20×10^{-5}	1.80×10^{-5}
50,200	2.55×10^{-5}	1.78×10^{-5}
51,200	2.62×10^{-5}	1.90×10^{-5}
52,800	3.20×10^{-5}	2.52×10^{-5}

Again referring to Figures 8 through 13, it will be observed that the plot of the experimental data approximates the fourth power relationship until the value of cyclic K reaches 0.7 to 0.8 of the K_c of the material. At this point, the linear plot of $\gamma = 4$ predicts a very rapid rate of crack growth. However, the experimental curves show a rate of crack growth even greater than that predicted by Equation 5. This behavior is very important in that it predicts an extremely rapid growth of the fatigue crack toward the end of the life of the structure.

To further study this behavior, a fractographic examination was conducted on the 1/4 inch thick specimen of 250 grade maraging steel cycled at a constant value of K. Typical fractographs taken from this specimen are shown in Figures 16 and 17.

It was observed that the fracture surface was predominately covered with ductile rupture dimples and, to a much smaller degree, with a few fatigue striations. This seems to indicate that "pop-in" or unstable crack propagation ahead of the fatigue crack front may be

responsible for the observed acceleration in the fatigue crack propagation rate, which is greater than that predicted by Equation 5.

All of the experimental data for the high strength steels tested are summarized in Figure 18. In this figure, the line for a $\gamma = 4$ value is also shown. At the lower values of cyclic K, the data fall into a small scatter band around this line. This indicates that, in the steels investigated, the rate of crack propagation is relatively insensitive to alloying and processing, as well as to mean load, frequency, etc.[12] The deviation from the fourth power relationship was greatest at high K values, as discussed for each individual material.

From a design standpoint, it is of primary interest to develop a concept for predicting the low cycle fatigue behavior of structures fabricated from these steels. The functional form followed by the data presented, including the deviations discussed, is represented by

$$\frac{da}{dN} = f\ (K \text{ or } \Delta K) \tag{6}$$

where K is a function of σ and the geometrical configuration of the body, including the crack a. Equation 5 is a more limited representation of the form of Equation 6 not including the deviations.

By rearranging terms, it is possible to integrate either Equation 5 or Equation 6 as follows:

$$\int_{a_o}^{a_{cr}} \frac{da}{f(K \text{ or } \Delta K)} = \int_{o}^{N_F} dN \tag{7}$$

The right hand side of this equation becomes N_F, but the left hand side requires either a numerical integration using the experimental data in the form of Equation 6 (as on Figures 8 through 13 and Figure 18), or an analytical integration making use of Equation 5.

The numerical integrations were performed by programing the data for computer calculations. Also, an analytical integration was carried out for a small crack in an infinite membrane using Equation 5, the simple fourth power relation. The resulting expression is given as

$$N_F = \frac{1}{C_1 \sigma^2 K_c{}^2} \left(\frac{a_{cr}}{a_o} - 1 \right) \tag{8}$$

The effect upon the number of cycles to failure after adjusting for the deviation from the fourth power relationship through numerical integration is illustrated in Table IV. The sample calculations were performed using data for the 0.250 inch thick 250 grade maraging steel.

TABLE IV. Theoretical Cyclic Life of 250 Grade Maraging Steel

Stress (psi)	Initial Crack Length (in.)	Number of Cycles to Failure		Percent Differential
		Model 1[a]	Model 2[b]	
180,000	0.06	1,000	500	50
180,000	0.18	230	50	78
100,000	0.06	13,000	5,600	57
100,000	0.18	3,900	2,200	44

[a]Model 1 - Analytical integration
[b]Model 2 - Numerical integration

These calculations show that it is possible to induce relatively large errors in the predicted life of a structure by not allowing for the deviation from the fourth power relationship, even at relatively low operating stresses.

CONCLUSIONS

It may be concluded that

1. At high values of cyclic K, the rate of crack propagation deviates from the fourth power relationship and shows a higher rate of crack propagation than would be predicted.

2. Both the tempered martensitic and the maraging type of steels conform to this behavior.

3. Electron microfractographs taken along the path of fatigue crack growth show essentially the same rate of crack extension as that determined macroscopically.

RECOMMENDATIONS

It is recommended that

1. Additional low cycle fatigue work be conducted, using a single material and specimen thickness, in an effort to minimize scatter by refining the techniques used in this investigation.

2. Additional work be performed to determine the effects of frequency, mean load, temperature, and environment on the low cycle fatigue properties of various materials.

3. Further studies be conducted on the technique of numerical integration for predicting the life of structures.

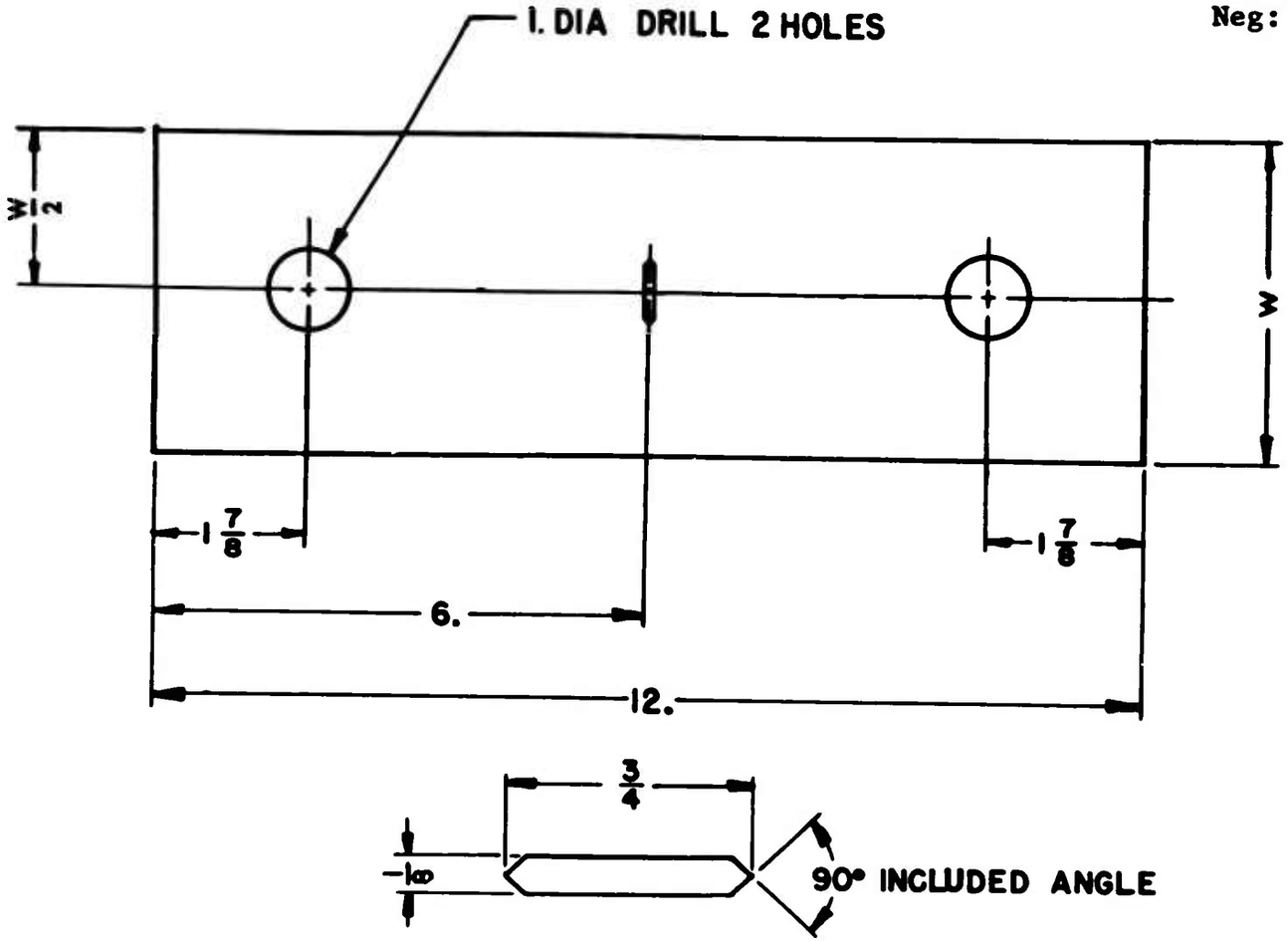

THICKNESS OF SPECIMEN IS SAME AS MATERIAL SUPPLIED

Figure 1. Drawing of Center-cracked Fracture Toughness and Fatigue Specimen

Neg: 36.231.S0367/AMC.66

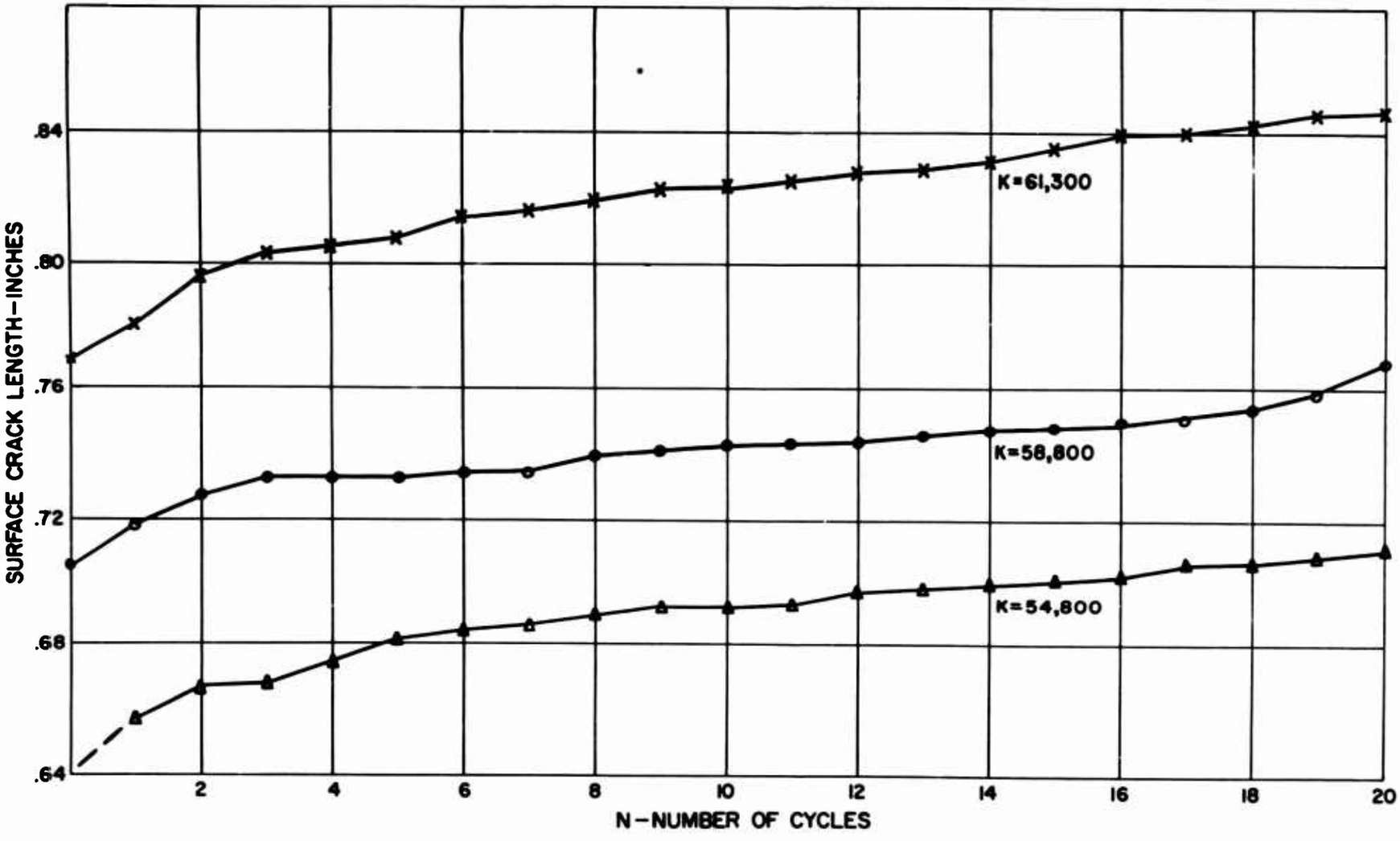

Figure 2. Crack Length vs Cycle Curves for D6Ac Steel (0.160 inch), Cycled at a Constant Value of K

Neg: 36.231.S0370/AMC.66

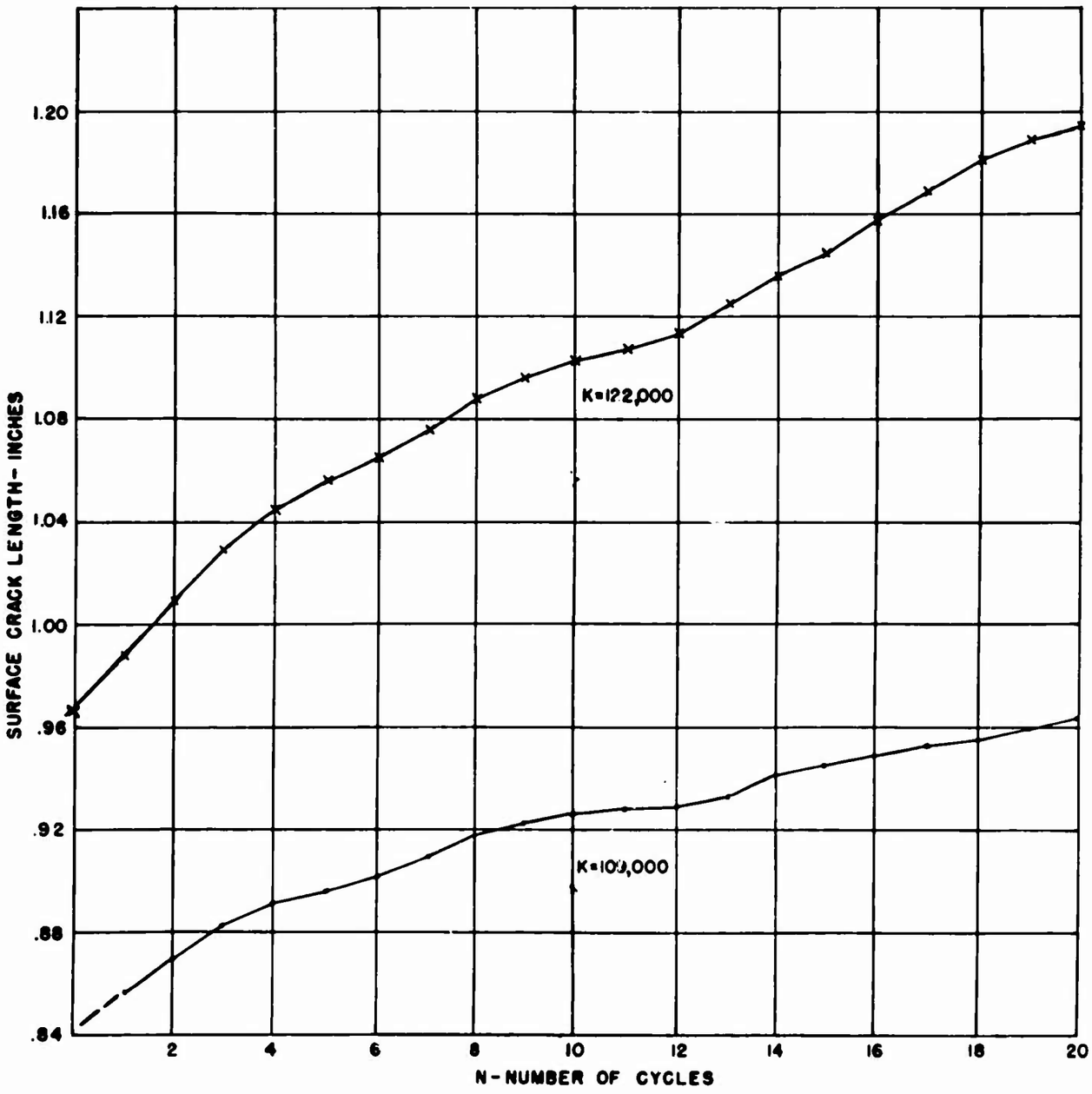

Figure 3. Crack Length vs Cycle Curves for D6Ac Steel (0.077 inch), Cycled at a Constant Value of K

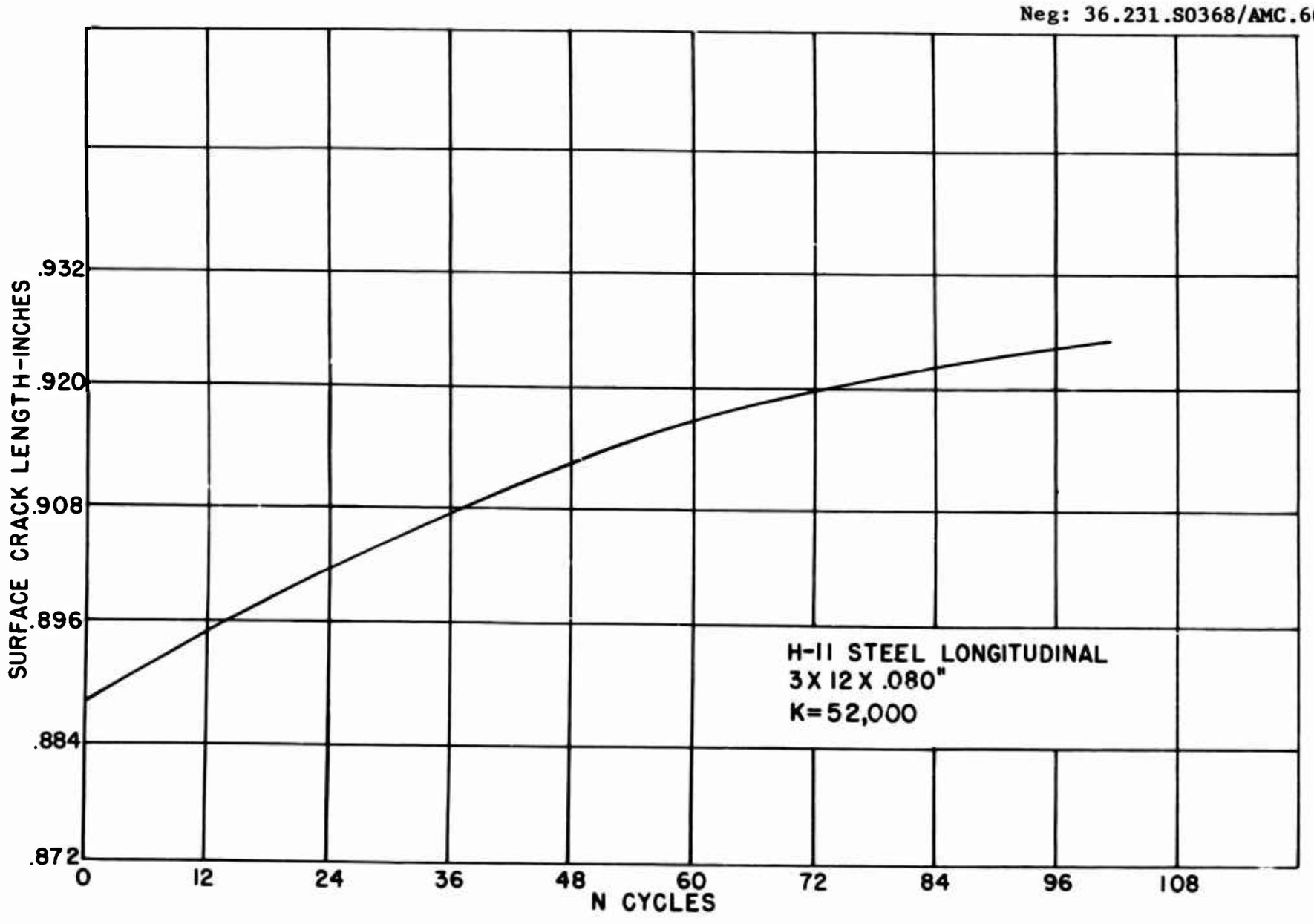
Neg: 36.231.S0368/AMC.66
SURFACE CRACK LENGTH-INCHES
.932
.920
.908
.896
.884
.872
0
12
24
36
48
60
72
84
96
108
N CYCLES
H-11 STEEL LONGITUDINAL
3 X 12 X .080"
K=52,000

Neg: 36.231.S0366/AMC.66

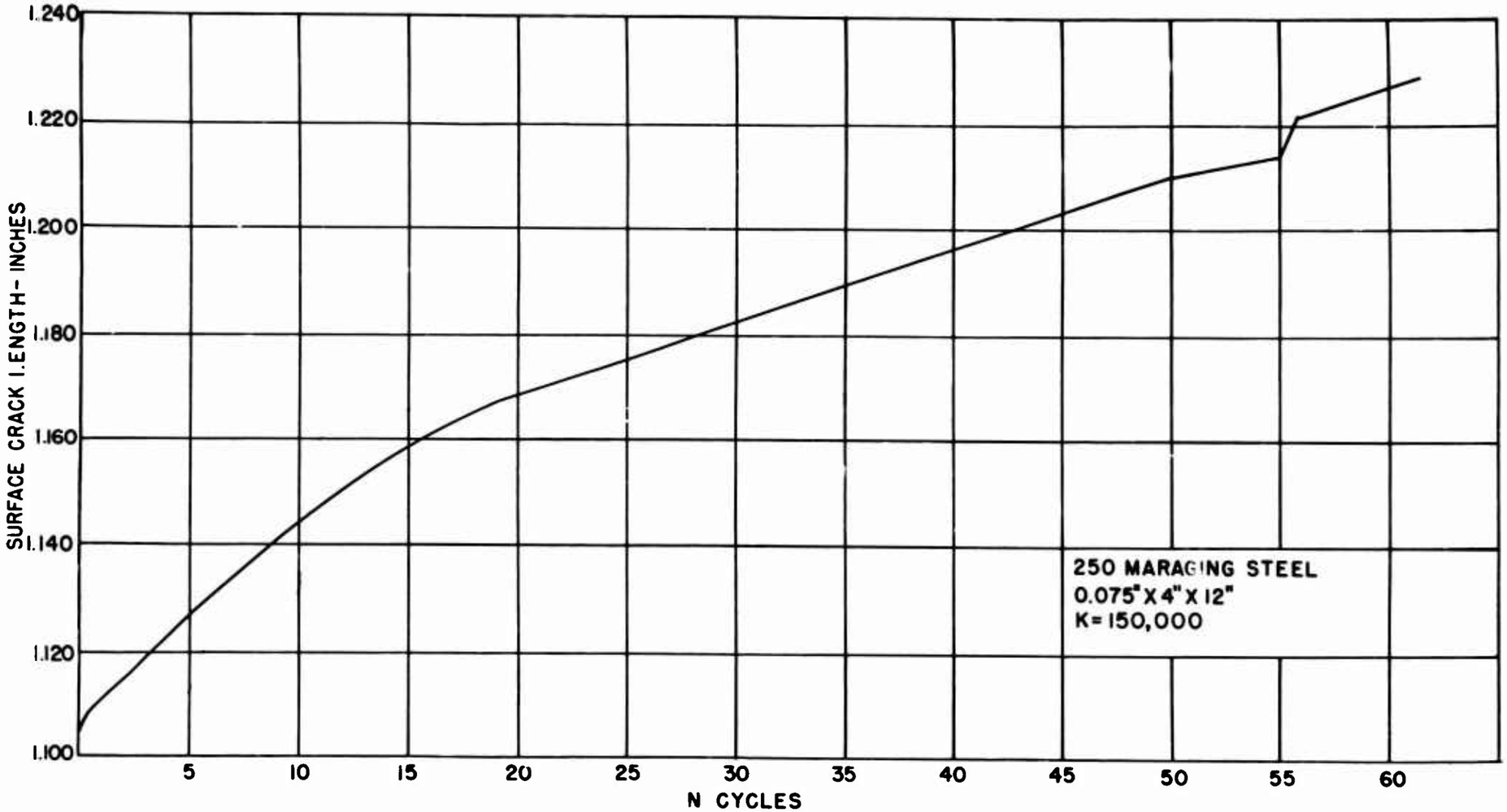

Figure 5. Typical Crack Length vs Cycle Curve for 250 grade Maraging Steel (0.075 inch), Cycled at a Constant Value of K

Neg: 36.231.S2323/AMC.64

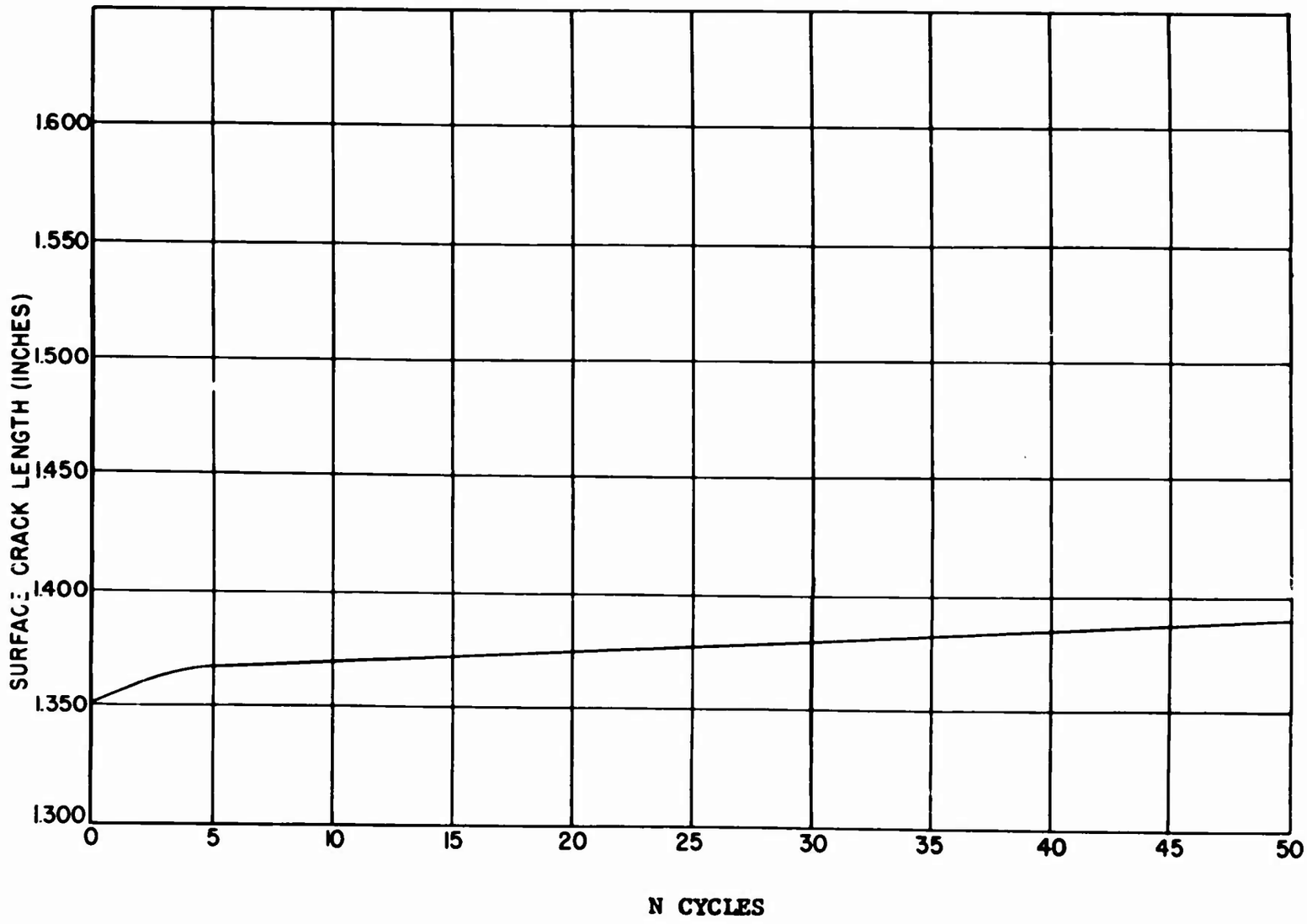

Figure 6. Typical Crack Length vs Cycle Curve for 250 grade Maraging Steel (0.250 inch), Cycled at a Constant Value of K

Neg: 36.231.S2324/AMC.64

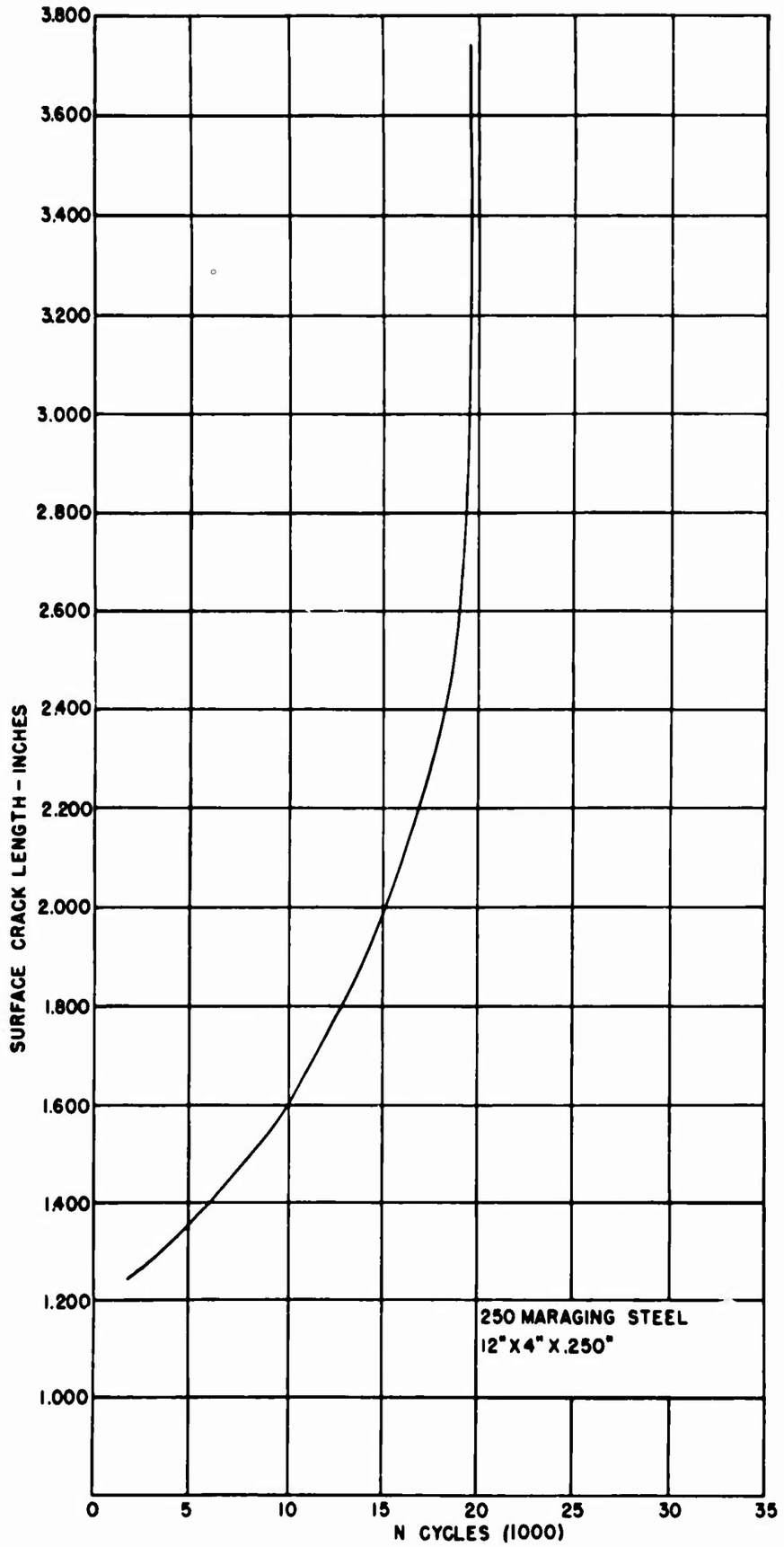

Figure 7. Typical Crack Length vs Cycle Curve for 250 grade Maraging Steel (0.250 inch), Cycled at Constant Stress (σ = 31,500 psi)

Neg: 36.231.S0369/AMC.66

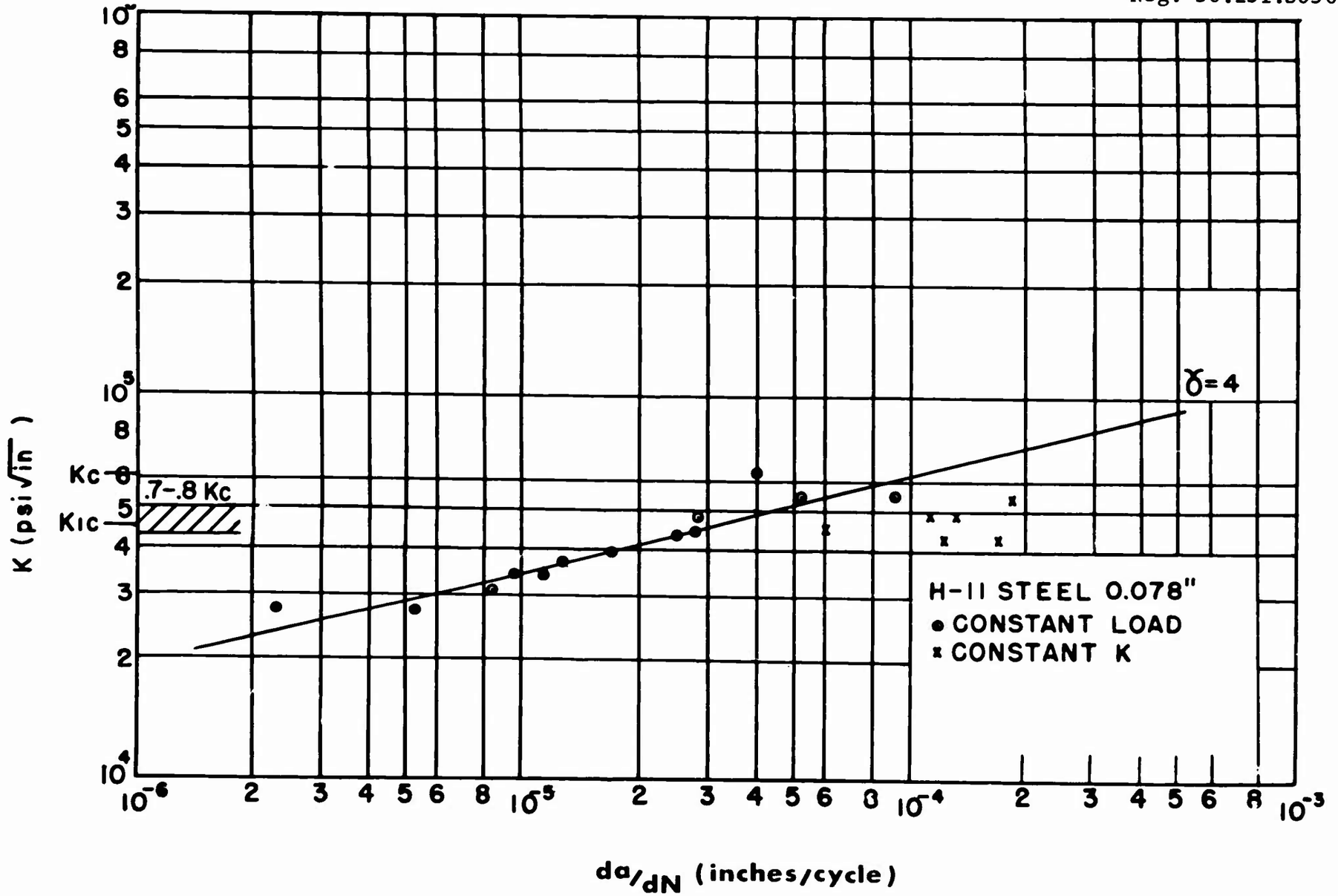

Figure 8. Crack Growth Rate as a Function of K for H11 Steel

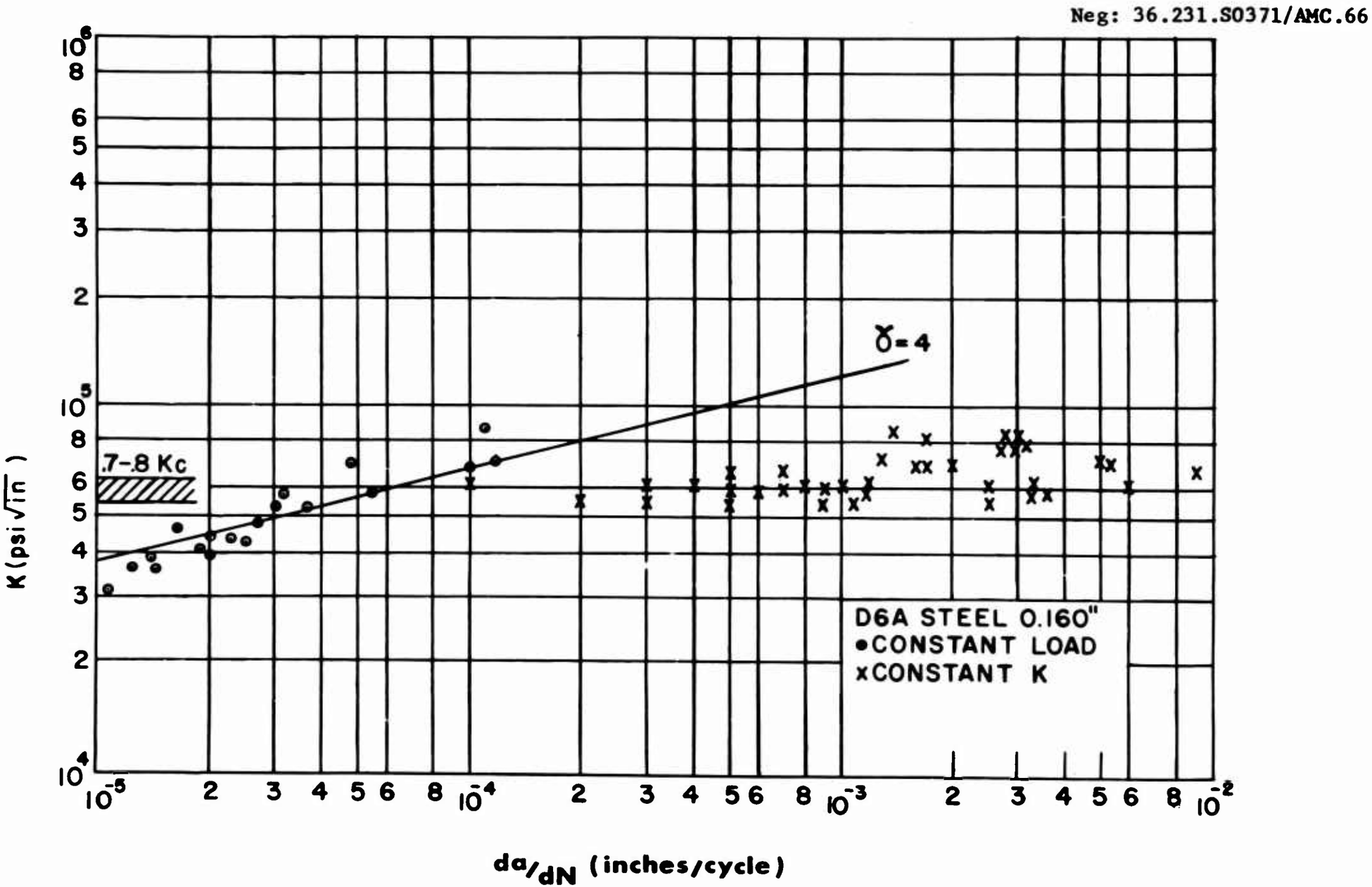

Figure 9. Crack Growth Rate as a Function of K for D6Ac Steel (0.160 inch thick)

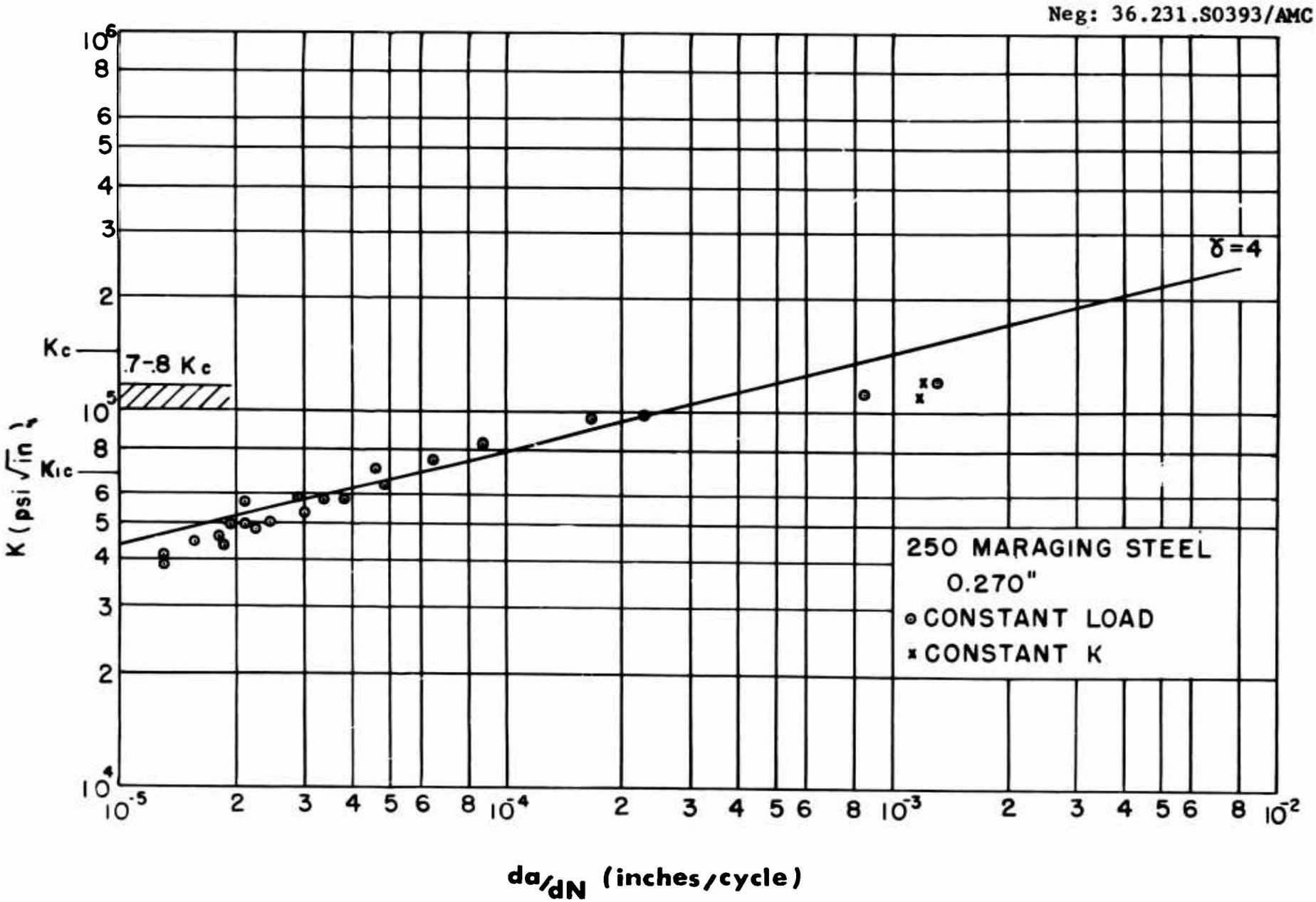

Figure 10. Crack Growth Rate as a Function of K for 250 grade Maraging Steel (0.270 inch thick)

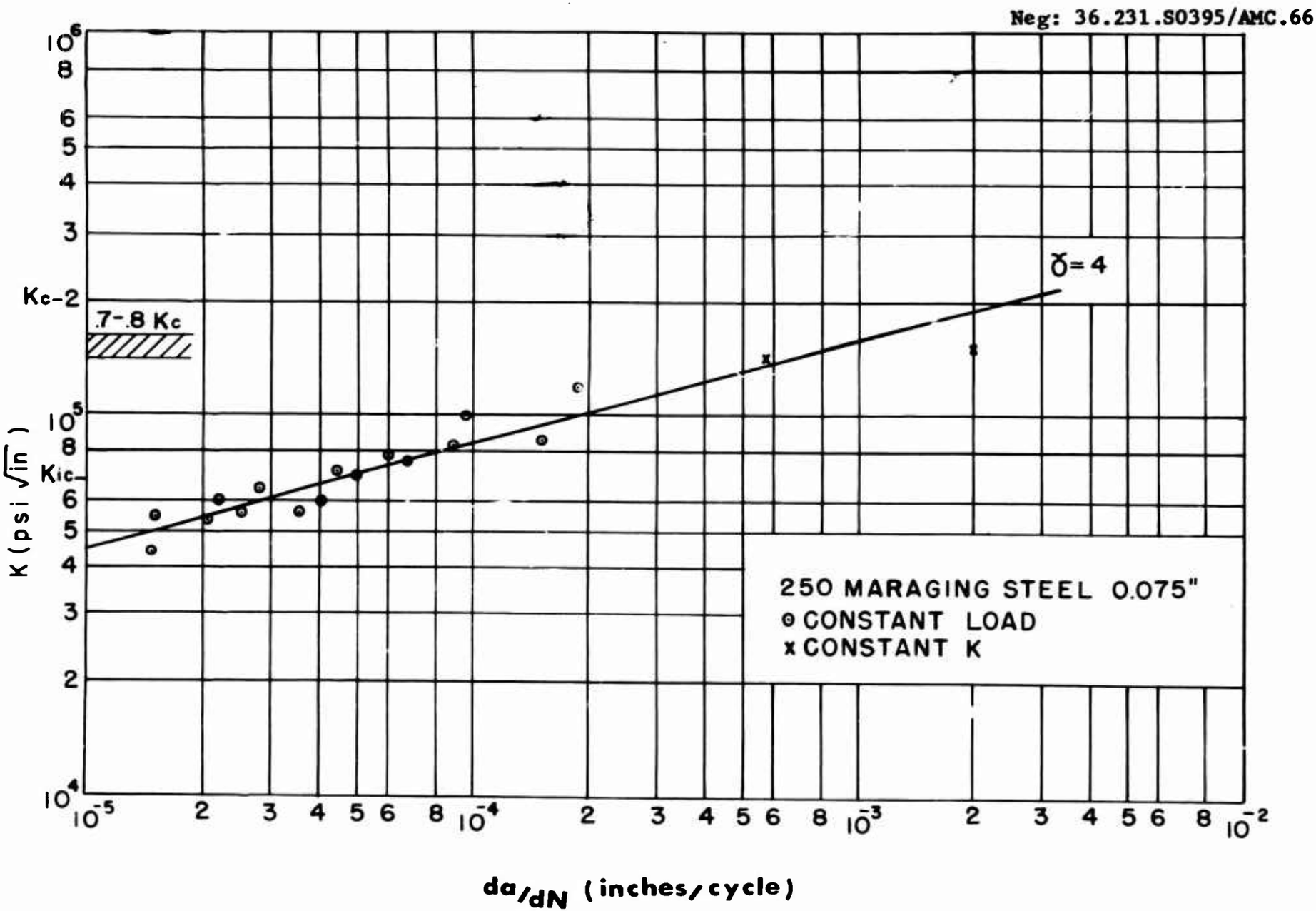

Figure 11. Crack Growth Rate as a Function of K for 250 grade Maraging Steel (0.075 inch thick)

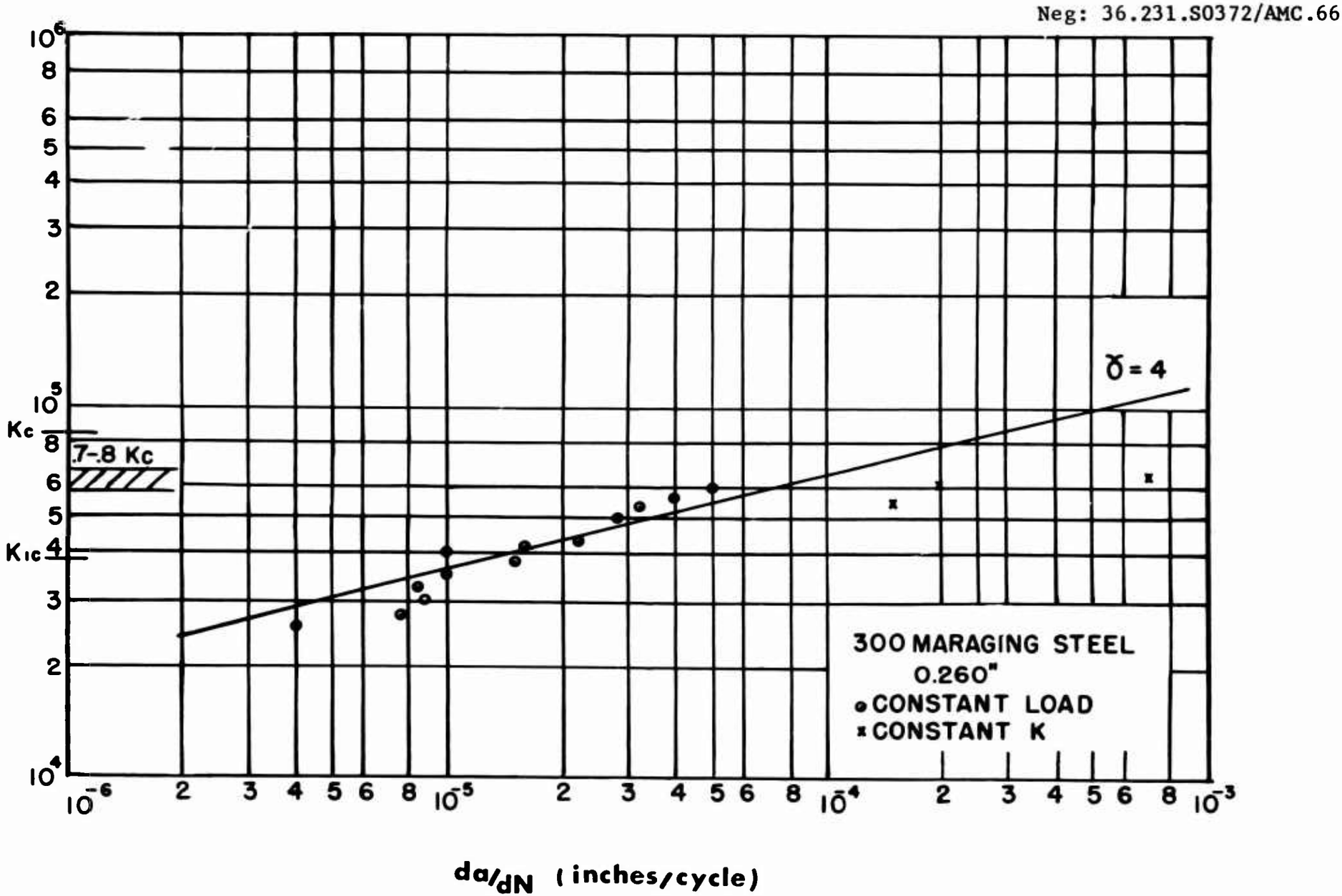

Figure 12. Crack Growth Rate as a Function of K for 300 grade Maraging Steel (0.260 inch thick)

Neg: 36.231.S0396/AMC.66

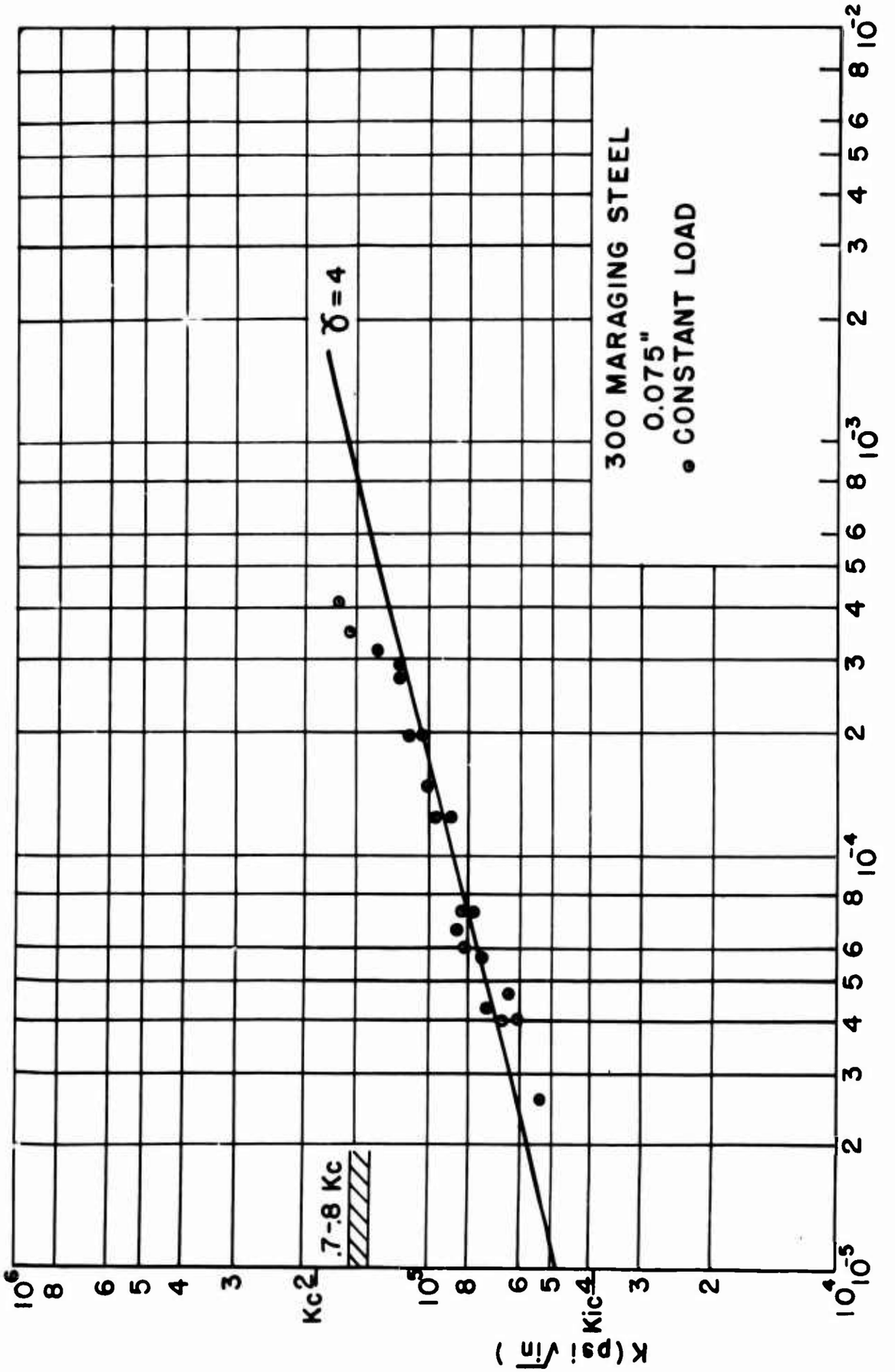

Figure 13. Crack Growth Rate as a Function of K for 300 grade Maraging Steel (0.075 inch thick)

Neg: 36.231.S2568/AMC.64

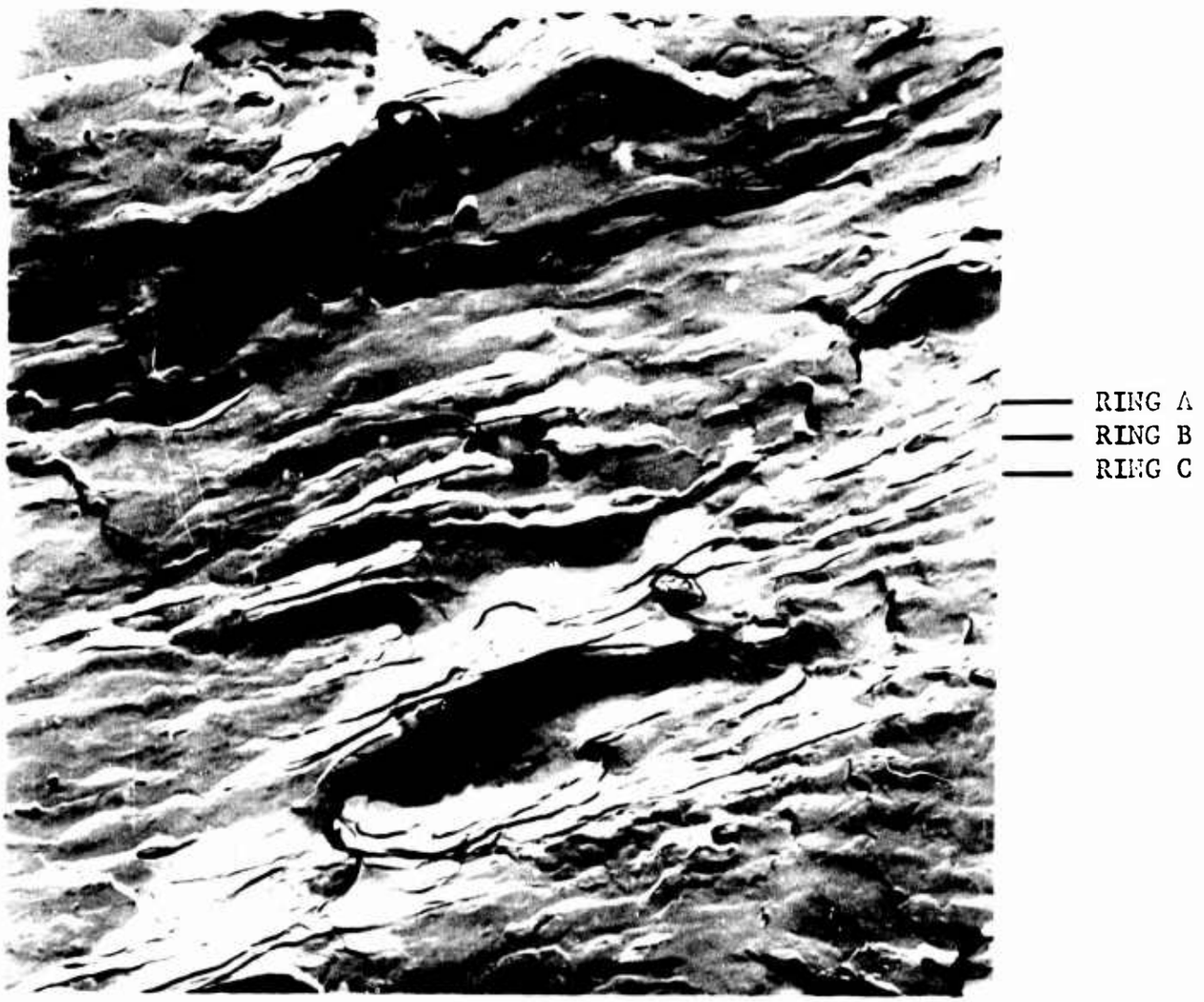

Two-stage replica 9250 X

Figure 14. Electron microfractograph showing Fatigue Growth Rings corresponding to a Crack Growth Rate of 1.77 x 10^{-5} inch per cycle at a K level of 50,200 psi $\sqrt{in}$.

Neg: 36.231.S2569/AMC.64

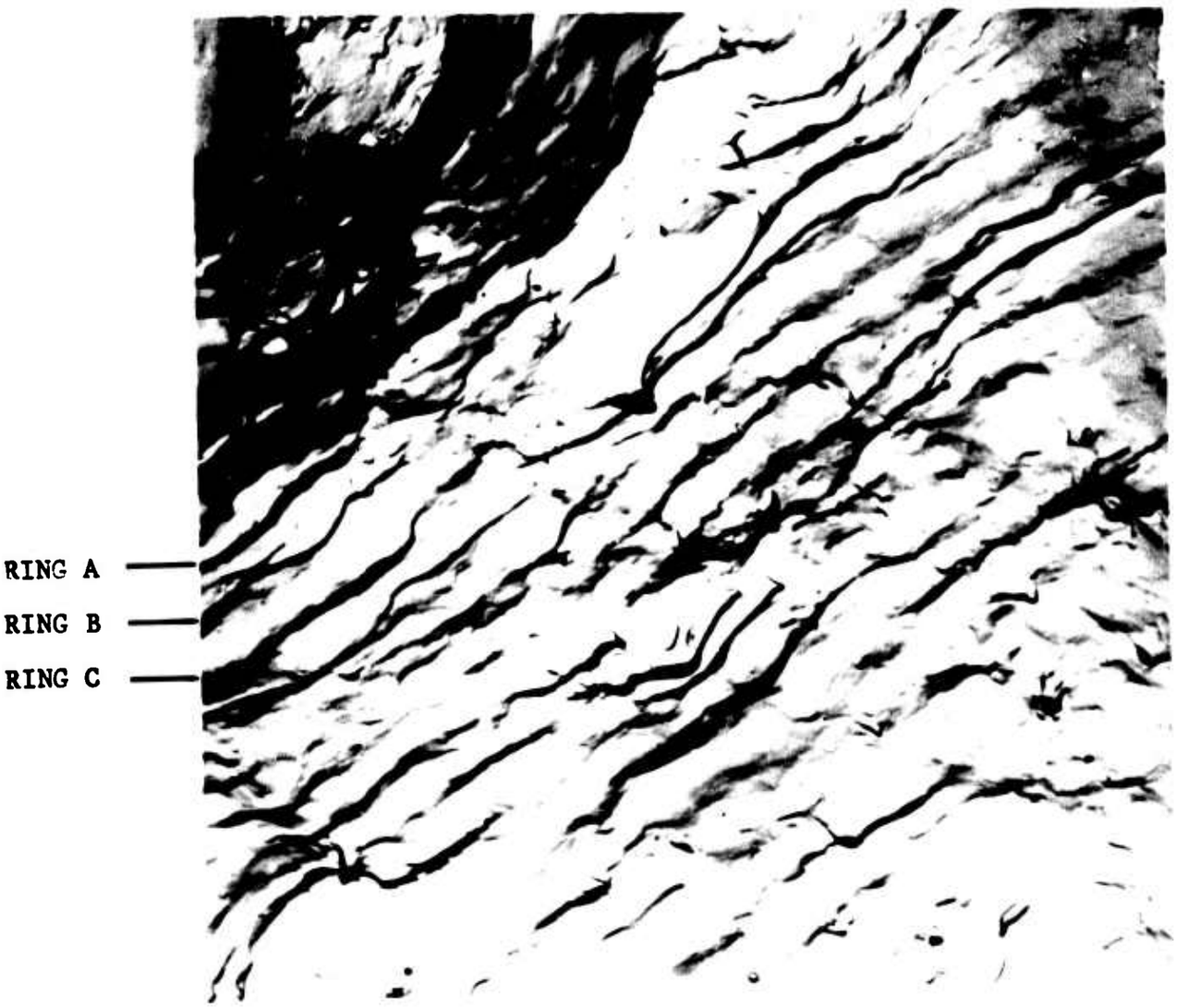

Two-stage replica 9250 X

Figure 15. Electron microfractograph showing Fatigue Growth Rings corresponding to a Crack Growth Rate of 2.38 x 10^{-5} inch per cycle at a K level of 52,800 psi $\sqrt{in.}$

Neg: 36.231.S0301/AMC.66

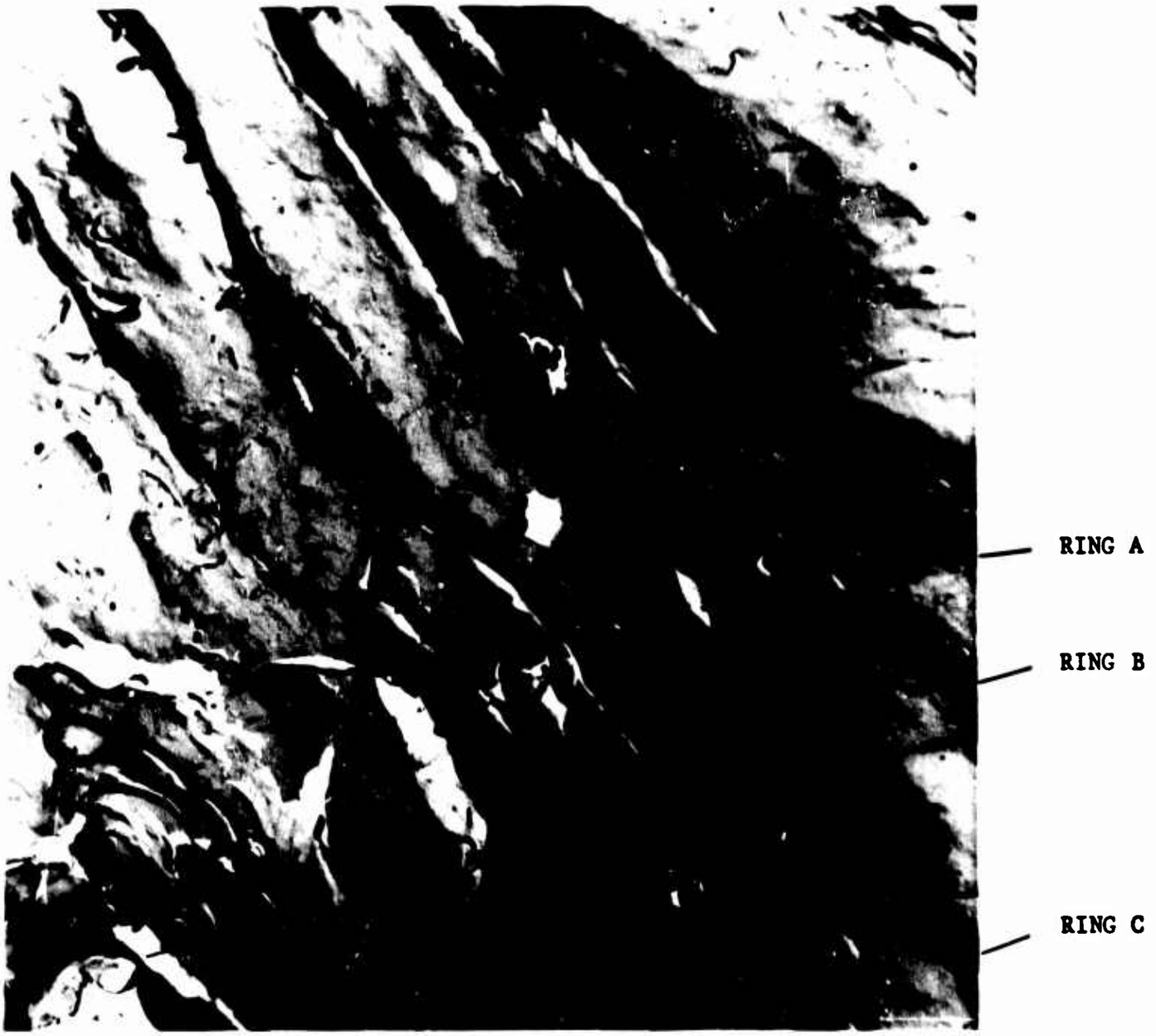

Figure 16. Electron microfractograph showing Fatigue Growth Striations observed in Specimen of 250 grade Maraging Steel Cycled at Constant K

Neg: 36.231.S0302/AMC.66

4430 X

Figure 17. Electron microfractograph showing Ductile Rupture Dimples observed in Specimen of 250 grade Maraging Steel Cycled at Constant K

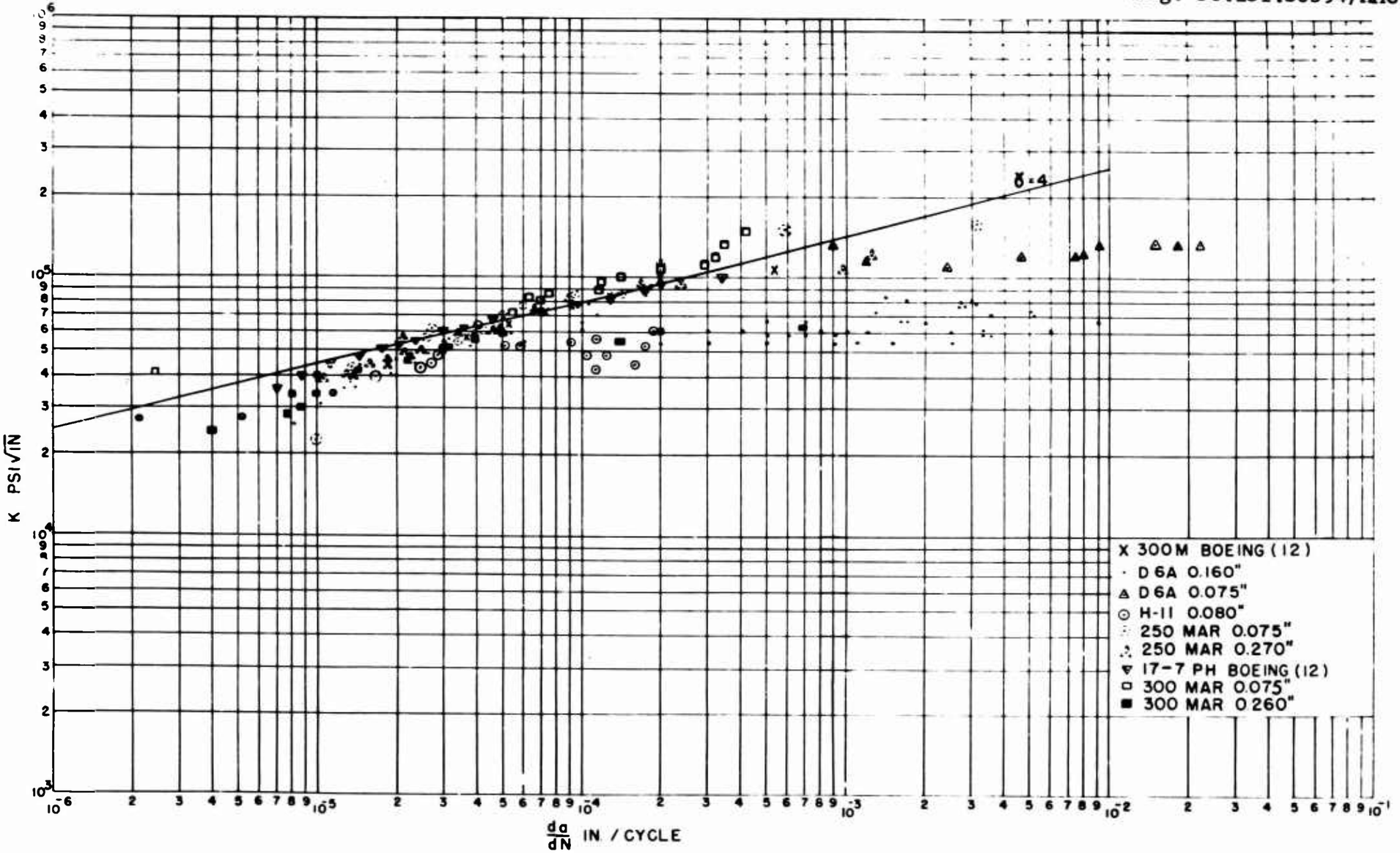

Figure 18. Crack Growth Rate as a Function of K for a Variety of Steels

REFERENCES

1. R. W. Boyle, A. M. Sullivan, and J. M. Krafft, "Determination of Plane Strain Fracture Toughness with Sharply Notched Sheets," Welding Journal (Research Supplement), Vol 41, No. 9, pp 428s-432s, Sep 1962.

2. G. R. Irwin, "Fracture Mode Transition for a Crack Traversing a Plate," Trans ASME, Vol 82, Series D, No. 2, Jun 1960.

3. A. K. Head, "The Growth of Fatigue Cracks," The Philosophical Magazine, Vol 44, series 7, p 925, 1953.

4. N. E. Frost and D. S. Dugdale, "The Propagation of Fatigue Cracks in Sheet Specimens," Journal of the Mechanics and Physics of Solids, Vol 6, No. 2, p 92, 1958.

5 H. W. Liu, "Fatigue Crack Propagation and Applied Stress Range - An Energy Approach," Trans ASME, Vol 85, Series D, No. 1, Mar 1963.

6. G. R. Irwin, "Fracture Testing of High Strength Sheet Materials Under Conditions Appropriate for Stress Analysis," Naval Research Laboratory Report No. 5486, July 1960.

7. M. Greenspan, "Axial Rigidity of Perforated Structural Members," NBS Journal of Research, Vol 31, Dec 1943.

8. P. C. Paris and F. Erdogan, "Critical Analysis of Crack Propagation Laws," Trans ASME, Vol 85, Series D, No. 4, Dec 1963.

9. R. M. N. Pelloux, "Influence of Constituent Particles on Fatigue Crack Propagation in Aluminum Alloys," Boeing Scientific Research Laboratories, Doc D1-82-079, Sep 1963.

10. R. W. Hertzberg and P. Paris, "Application of Electron Fractography and Fracture Mechanis to Fatigue Crack Propagation," Proceedings of the International Conference on Fracture (Sendai, Japan), Sep 1965.

11. M. Schuler and C. M. Carman, "Low Cycle Fatigue Properties of 18 NiCoMo 250 Maraging Steel," Notes for Meeting of Subcommittee on Metallography and Fractography of ASTM Committee E-24 (Schnectady, N.Y.), Oct 1964.

12. D. R. Donaldson and W. E. Anderson, "Crack Propagation Behavior of some Airframe Materials," Crack Propagation Symposium (Cranfield, Englan), Sep 1961.

UNCLASSIFIED
Security Classification

DOCUMENT CONTROL DATA - R&D

(Security classification of title, body of abstract and indexing annotation must be entered when the overall report is classified)

1. ORIGINATING ACTIVITY (Corporate author) FRANKFORD ARSENAL, Philadelphia, Pa. 19137 (SMUFA L3300)	2a. REPORT SECURITY CLASSIFICATION Unclassified 2b GROUP NA

3. REPORT TITLE

Low Cycle Fatigue Crack Propagation Characteristics of High Strength Steels

4. DESCRIPTIVE NOTES (Type of report and inclusive dates)

Technical research report

5. AUTHOR(S) (Last name, first name, initial)

CARMAN, Carl M.
KATLIN, Jesse M.

6. REPORT DATE	7a TOTAL NO. OF PAGES	7b. NO. OF REFS
April 1966	36	12

8a. CONTRACT OR GRANT NO.	9a. ORIGINATOR'S REPORT NUMBER(S)
AMCMS Code 5025.11.294 b. PROJECT NO. DA Project 1C024401A328 c. d.	Frankford Arsenal Report R-1806 9b. OTHER REPORT NO(S) (Any other numbers that may be assigned this report)

10. AVAILABILITY/LIMITATION NOTICES

Distribution of this report is unlimited.

11. SUPPLEMENTARY NOTES	12. SPONSORING MILITARY ACTIVITY
	AMCRD-RC

13. ABSTRACT

The fatigue crack growth properties of various high strength steels, including the 250 and 300 grades of the 18Ni-Co-Mo maraging steel, H11 steel, and D6A steel, have been studied using a center-cracked specimen. Experiments were conducted by cycling either at a constant stress or at a constant value of the stress intensity parameter, K.

A log-log plot of da/dN as a function of K for these steels resulted in a straight line having a slope of four. The data exhibited normal scatter about this straight line. These data are in agreement with the relationship $da/dN = (\Delta K)^4 M$ as proposed by Paris. A departure from this relation to higher rates was observed at values of cyclic K equal to 0.7 to 0.8 of static K_c.

Electron microfractographs taken along the path of fatigue crack extension in the 250 grade maraging steel showed the growth ring pattern characteristic of fatigue. Measurement of the growth ring spacings and knowledge of the crack length permit calculation of the rate of crack extension as a function of K. The rates of crack extension, as determined by fractography and actual measurement on the specimen, are in good agreement.

A technique for calculating the cyclic life of structures involving a numerical integration of K as a function of crack length and stress was programmed for computer operation. This calculation allows for the change in slope of the K vs da/dN at higher values of cyclic K. The results of these calculations are compared with the life prediction made by simple mathematical integration of the fourth power relationship for an infinite plate.

DD FORM 1 JAN 64 1473

UNCLASSIFIED
Security Classification

14. KEY WORDS	LINK A		LINK B		LINK C	
	ROLE	WT	ROLE	WT	ROLE	WT
Iron Alloys Steels Fracture Mechanics Fatigue Fracture						

INSTRUCTIONS

1. ORIGINATING ACTIVITY: Enter the name and address of the contractor, subcontractor, grantee, Department of Defense activity or other organization *(corporate author)* issuing the report.

2*a*. REPORT SECURITY CLASSIFICATION: Enter the overall security classification of the report. Indicate whether "Restricted Data" is included. Marking is to be in accordance with appropriate security regulations.

2*b*. GROUP: Automatic downgrading is specified in DoD Directive 5200.10 and Armed Forces Industrial Manual. Enter the group number. Also, when applicable, show that optional markings have been used for Group 3 and Group 4 as authorized.

3. REPORT TITLE: Enter the complete report title in all capital letters. Titles in all cases should be unclassified. If a meaningful title cannot be selected without classification, show title classification in all capitals in parenthesis immediately following the title.

4. DESCRIPTIVE NOTES: If appropriate, enter the type of report, e.g., interim, progress, summary, annual, or final. Give the inclusive dates when a specific reporting period is covered.

5. AUTHOR(S): Enter the name(s) of author(s) as shown on or in the report. Enter last name, first name, middle initial. If military, show rank and branch of service. The name of the principal author is an absolute minimum requirement.

6. REPORT DATE: Enter the date of the report as day, month, year; or month, year. If more than one date appears on the report, use date of publication.

7*a*. TOTAL NUMBER OF PAGES: The total page count should follow normal pagination procedures, i.e., enter the number of pages containing information.

7*b*. NUMBER OF REFERENCES: Enter the total number of references cited in the report.

8*a*. CONTRACT OR GRANT NUMBER: If appropriate, enter the applicable number of the contract or grant under which the report was written.

8*b*, 8*c*, & 8*d*. PROJECT NUMBER: Enter the appropriate military department identification, such as project number, subproject number, system numbers, task number, etc.

9*a*. ORIGINATOR'S REPORT NUMBER(S): Enter the official report number by which the document will be identified and controlled by the originating activity. This number must be unique to this report.

9*b*. OTHER REPORT NUMBER(S): If the report has been assigned any other report numbers *(either by the originator or by the sponsor)*, also enter this number(s).

10. AVAILABILITY/LIMITATION NOTICES: Enter any limitations on further dissemination of the report, other than those imposed by security classification, using standard statements such as:

(1) "Qualified requesters may obtain copies of this report from DDC."

(2) "Foreign announcement and dissemination of this report by DDC is not authorized."

(3) "U. S. Government agencies may obtain copies of this report directly from DDC. Other qualified DDC users shall request through _____."

(4) "U. S. military agencies may obtain copies of this report directly from DDC. Other qualified users shall request through _____."

(5) "All distribution of this report is controlled. Qualified DDC users shall request through _____."

If the report has been furnished to the Office of Technical Services, Department of Commerce, for sale to the public, indicate this fact and enter the price, if known.

11. SUPPLEMENTARY NOTES: Use for additional explanatory notes.

12. SPONSORING MILITARY ACTIVITY: Enter the name of the departmental project office or laboratory sponsoring *(paying for)* the research and development. Include address.

13. ABSTRACT: Enter an abstract giving a brief and factual summary of the document indicative of the report, even though it may also appear elsewhere in the body of the technical report. If additional space is required, a continuation sheet shall be attached.

It is highly desirable that the abstract of classified reports be unclassified. Each paragraph of the abstract shall end with an indication of the military security classification of the information in the paragraph, represented as *(TS)*, *(S)*, *(C)*, *or (U)*.

There is no limitation on the length of the abstract. However, the suggested length is from 150 to 225 words.

14. KEY WORDS: Key words are technically meaningful terms or short phrases that characterize a report and may be used as index entries for cataloging the report. Key words must be selected so that no security classification is required. Idenfiers, such as equipment model designation, trade name, military project code name, geographic location, may be used as key words but will be followed by an indication of technical context. The assignment of links, rules, and weights is optional.